

1 **Physical modeling of a stepped spillway without**  
2 **sidewalls**

3 S. Estrella<sup>1</sup>, M. Sánchez-Juny<sup>2</sup>, E. Bladé<sup>3</sup>, J. Dolz<sup>4</sup>

4

5

6

7 Word count: 3946 words + 12 figures (250 words/fig), 6946 words

8

---

<sup>1</sup> *Researcher, FLUMEN Institute, CIMNE and UPC BARCELONATECH, Jordi Girona 1-3, Building D1, Office 206, 08034, Barcelona, Spain. E-mail: soledad.estrella@upc.edu*

<sup>2</sup> *Associate professor, FLUMEN Institute, CIMNE and UPC BARCELONATECH, Jordi Girona 1-3, Building D1, Office 207, 08034, Barcelona, Spain. (Corresponding author). E-mail: marti.sanchez@upc.edu*

<sup>3</sup> *Assistant Professor, FLUMEN Institute, CIMNE and UPC BARCELONATECH, Jordi Girona 1-3, Building D1, Office 207, 08034, Barcelona, Spain. E-mail: ernest.blade@upc.edu*

<sup>4</sup> *Full professor, FLUMEN Institute, CIMNE and UPC BARCELONATECH, Jordi Girona 1-3, Building D1, Office 213, 08034, Barcelona, Spain. E-mail: j.dolz@upc.edu*

## 9 Abstract

10 The interest of a consulting company in designing stepped spillways in RCC dams led us to  
11 propose the possibility of building this type of spillway without sidewalls. Previous research on  
12 stepped spillways has focused on characterizing the complex hydraulic behavior of flow on these  
13 structures, as well as design criteria. Such studies have usually been conducted on stepped  
14 spillways with a constant width along the spillway, that is, with sidewalls.

15 In the present work, we report the results of the physical modeling of a generic stepped spillway  
16 without sidewalls (slope 1v:0.8h). In general terms, the lack of sidewalls produces a lateral  
17 expansion of water and therefore a non-uniform longitudinal and transversal discharge  
18 distribution. Consequently, the flow type, characteristic water depth, velocity, air concentration  
19 and pressure fields change along and across the spillway. The resulting data demonstrate that the  
20 distribution of the different variables studied depend on the specific discharge at the entrance and  
21 the spillway height.

## 22 1. Introduction

23 Since the early 1990s, empirical evidence on stepped spillways with sidewalls (Rajaratnam, 1990;  
24 Peyras et al. 1992) has identified two main flow types: skimming flow and nappe flow, and a  
25 transitional flow between these two. Later, different authors have proposed expressions to  
26 characterize the onset of each flow type (Chanson 2001; Meireles 2004; Sánchez-Juny et al. 2005;  
27 Amador 2005; Renna et al. 2010). Amador (2005), proposed the following expressions:

$$\frac{y_c}{h} = 0.649 \cdot \left(\frac{h}{l}\right)^{-0.175} \quad (1)$$

$$\frac{y_c}{h} = 0.854 \cdot \left(\frac{h}{l}\right)^{-0.169} \quad (2)$$

28 Equation **Error! No s'ha trobat l'origen de la referència.** indicates the upper limit for the  
29 existence of nappe flow and equation **Error! No s'ha trobat l'origen de la referència.** indicates  
30 the start of skimming flow. As observed, the presence of one type of flow or other depends on the

31 geometrical characteristics of the spillway deriving from its slope ( $h$  is the step height and  $l$  is the  
32 step length) and the specific discharge at the entrance ( $y_c$  is the critical depth there). In the case  
33 of a stepped spillway without sidewalls, a crosswise change of flow type is produced depending  
34 on lateral reduction of the specific discharge.

35

36 Stepped spillways are characterized by the natural entrance of air at the so-called inception point,  
37 which is located further upstream than on conventional smooth spillways (Boes and Minor, 2001).  
38 Different authors have studied the inception point and proposed equations to characterize it  
39 (Amador et al. 2006a; Meireles et al. 2012; Hunt et al. 2013). In the case of stepped spillways  
40 without sidewalls, it has been found that the location of the inception point is practically  
41 unaffected by the absence of sidewalls. Nevertheless, downstream from the inception point, the  
42 lateral expansion of the flow affects the behavior of the two-phase flow with respect to its  
43 traditional behavior. Since the 1980s (Falvey 1980), air-water flow and self-aeration in stepped  
44 chutes has been widely studied. In these previous works, velocity profiles in uniform flow have  
45 been adjusted to a power law as in equation (3):

$$\frac{v}{v_{90}} = \left( \frac{y}{y_{90}} \right)^{1/N} \quad (3)$$

46 where  $y$  is distance, measured in the normal direction to the pseudo-bottom defined by the external  
47 edges of the steps;  $y_{90}$  is the characteristic water depth, corresponding to the perpendicular depth  
48 where air concentration is 0.90 (Matos, 2000; Boes and Hager, 2003),  $v_{90}$  is the velocity measured  
49 at this characteristic water depth and  $N$  is the adjustment coefficient. Different authors (Chanson  
50 1994b; Matos 2000; Matos et al. 2000) define  $N$  somewhere between 3.5 and 30 depending on  
51 the specific discharge, the step length and the slope. More recently (Relvas and Pinheiro 2011),  
52 define that for skimming flows  $N < 9$  and for transition and nappe flows  $N \geq 9$ .

53

54 Regarding mean air concentration, Boes et al. (2003) found that this parameter is around 0.22 at  
55 the inception point for a typical gravity dam chute of  $53^\circ$ , which agrees with the 0.20 found by  
56 Matos et al. (2000). Downstream of the inception point, Chanson et al. (2002) found mean air

57 concentration to range from 0.2 to 0.6. On the other hand, air concentration distributions follow  
58 an analytical solution of the air-bubble advective diffusion equation (4) (Chanson and Toombes,  
59 2001 and 2004; Gonzalez et al. 2005):

$$C = 1 - \tanh^2 \left( K' - \frac{y}{2 \cdot Do} + \frac{\left( \frac{y}{y_{90}} - \frac{1}{3} \right)^3}{3 \cdot Do} \right) \quad (4)$$

60 where  $y$  is the water depth measured normal to the pseudo-bottom,  $y_{90}$  is the characteristic water  
61 depth,  $K'$  is an integration constant (5) and  $Do$  is a function of the mean air concentration  $C_{med}$   
62 (6):

$$K' = 0.32745 + \frac{1}{2 \cdot Do} - \frac{8}{81 \cdot Do} \quad (5)$$

$$C_{med} = 0.762 \cdot (1.043 - \exp(-3.61 \cdot Do)) \quad (6)$$

63

64 The pressure field over the steps has been analyzed by several authors (Sánchez-Juny et al. 2003;  
65 Sánchez-Juny et al. 2007 and 2008; Amador et al. 2006b, 2009).

66

67 This paper presents empirical evidence for the behavior of a stepped spillway without sidewalls  
68 taking into account the hydraulic characteristics studied by the different authors mentioned above.

## 69 **2. Experimental overview**

70 The experimental data presented in this paper were recorded on a stepped chute model (Figure 1).

71 This chute is 5.26 m high (from crest to toe), with a slope of 1v:0.8h and a total width of 3.0 m.

72 It consists of 57 identical steps 0.08 m high ( $h$ ), 0.064 m long ( $l$ ) and 8 more steps at the top of

73 the model fitted to a Creager profile (Estrella, 2013). The model is built of transparent

74 methacrylate in order to allow visual inspection of the flow.

75

76 It is worth mentioning that the spill window is located on the right-hand side of the model in order  
77 to increase available expansion width. The maximum discharge tested is  $260 \text{ ls}^{-1}$ . Taking into  
78 account that the spill-width at the entrance of the chute is 1.0 m, the range of dimensionless  
79 discharge  $(y_c/h)_e$  varied from 0 to 2.37. All results presented in this article correspond to the test  
80 carried out with the maximum flow rate  $(y_c/h)_e=2.37$ .

81

82 Additionally, a guiding wall was located at the crest of the dam. Its length approximately  
83 represents a typical supporting pile of a possible access road usually present in this type of  
84 structure, around 10 m in prototype. Hydraulically, this wall guides the flow and provides an  
85 output velocity that reduces the lateral spread of water.

86

87 Transverse discharge distribution was measured by dividing the width of the chute into three  
88 separate channels: a right channel (faced to the spill window), a central channel and a left channel.  
89 Flow distribution at the dam toe was measured for different specific discharges  $(y_c/h)_e$ .  
90 Transversal flow distribution was obtained at the dam toe (step 62) as well as at different heights  
91 along the spillway (steps 22, 32, 42 and 52). Note that the guiding wall reaches step 12.

92

93 Local air concentration, velocity and characteristic water depth were measured with a double  
94 fiber-optical probe (RBI Instrumentation). A single-tip of the probe detects interfaces (i.e. the  
95 instant at which the tip passes from liquid to gas and from gas to liquid). A dual-tip probe can  
96 measure the delay necessary for an interface to travel between tip 1 and tip 2. Knowing the  
97 distance between the 2 tips, the velocity of the interface can be evaluated. Supposing a  
98 homogeneous flow, liquid velocity is assumed to be equal to the bubble velocity detected by the  
99 double fiber-optical probe. The probe used in this investigation has a distance of 2.5 mm between  
100 the 2 tips. Each acquisition test was stopped after 1 min or after detection of 50000 single air  
101 bubbles per probe tip, i.e. 1 min test was the main constrain. The bubble size registered usually  
102 ranged between 1.9 mm and 4 mm. More details of the measurement technique can be found in  
103 Boes and Hager (1998). Velocity and air concentration profiles were obtained in a perpendicular

104 direction to the pseudo-bottom, and the characteristic water depth was estimated as the position  
105 where the air concentration was 0.90.

106

107 Pressure measurements were recorded by means of piezoresistive transducers using an acquisition  
108 frequency of 100 Hz and data acquisition times of 60 secs. The range of measurement was from  
109 -1.5 to +2.0m with an error of  $\pm 0.0035\text{m}$  (Estrella, 2013).

## 110 **3. Results**

### 111 **3.1. Inception point**

112 In the case of stepped spillways without sidewalls, it has been found that the location of the  
113 inception point is practically unaffected by the absence of sidewalls. As can be observed in Figure  
114 2, the result is similar to that proposed by Amador et al. (2006a) and Meireles et al. (2012).

### 115 **3.2. Flow distribution**

116 In stepped spillways without sidewalls, the entire dam width can be used for flow spill. As can be  
117 observed in Figure 1, downstream from the guiding wall, the flow experiences a lateral expansion  
118 (Figure 3) and the specific discharge therefore decreases across the spillway. Experiments  
119 (detailed in Estrella, 2013) have shown that this reduction is mostly dependent on the specific  
120 discharge at the entrance  $(y_c/h)_e$  and the spillway height  $(L/L_t)$ .

121

122 Figure 4 exemplifies the flow distribution measured in the case of  $b_0/B=1/3$  and for the case of a  
123 dimensionless discharge at the crest  $(y_c/h)_e$  of 1.14, 1.56 and 2.06. Estrella et al. (2011) present  
124 results for other conditions of  $b_0/B$  and  $(y_c/h)_e$ .

125

126 The transversal flow regime can be characterized along the spillway. Figure 5 shows the  
127 transversal limits of each flow type observed for different  $(y_c/h)_e$  (observed data) as well as the  
128 limits calculated with the expressions proposed by Amador (2005) for the corresponding specific

129 discharge (adjustment). In this case, nappe flow will occur for  $y_c/h < 0.62$  and skimming flow for  
130  $y_c/h > 0.82$ .

131

132 Depending on the discharge and the dam widths at the top and at the toe, and also the dam height,  
133 the flow can reach the lateral abutments, or not. The risk of local scour there can be analyzed by  
134 the designer depending on the geology of the abutment using the estimated discharge obtained  
135 from the figure 3.

### 136 **3.3. Characteristic water depth**

137 The following figures show the evolution of normalized characteristic water depth ( $y_{90}/(y_{90})_{qe}$ )  
138 along the dimensionless length of the spillway ( $L/L_t$ ). Results are normalized with respect to the  
139 characteristic water depth in the zone not affected by the lack of sidewalls, that is, the zone where  
140 the specific discharge is the same as that at the entrance to the chute ( $(y_{90})_{qe}$ ).

141

142 Figure 6 shows the case  $(y_c/h)_e = 2.37$ . The dependence of characteristic water depth on transversal  
143 position ( $x/B$ ) and on specific discharge ( $q/q_e$ ) is presented for different values of spillway length.

144

145 Characteristic water depth decreases as the flow expands across the chute (increasing  $x/B$ ) and  
146 the specific discharge decreases ( $q/q_e$ ), regardless of the longitudinal position on the spillway  
147 ( $L/L_t$ ). A reduction of 50% in flow rate produces a 40% reduction of the characteristic water depth  
148 with respect to that in the zone not affected by flow expansion.

### 149 **3.4. Velocity field**

150 The following figures illustrate the results of the normalized velocity profiles  $v/v_{90}$  as a function  
151 of  $y/y_{90}$ , where  $V_{90}$  is the characteristic interfacial velocity where  $C=0.9$ . Figure 7 shows the  
152 normalized velocity profiles for different flow rates  $(y_c/h)_e$ , at  $L/L_t=0.95$  close to the spillway toe  
153 (step 58). Across the chute, profiles were obtained at sections  $x/B=0, 1/10, 1/6$ .

154

155 Coefficients  $N$  of the equation (3) were obtained from the recorded velocity profiles. Figure 8  
156 shows the longitudinal evolution of  $N$  for the tests with specific discharge at the entrance  
157  $(y_c/h)_e=2.37$ .  $N$  increases as the flow expands, although its value ranges between 3 and 5. Close  
158 to the spillway toe, at  $x/B=1/6$  the flow rate is within the range of transitional flow and the  
159 exponent  $N$  reaches values higher than 10. This is coherent with Relvas and Pinheiro (2011).

### 160 **3.5. Air concentration**

161 In the case of the stepped spillway without sidewalls, the area not affected by flow expansion  
162 presented mean air concentrations of between 0.32 and 0.59 in the different experiments carried  
163 out, exhibiting an increment downstream from the inception point in accordance with the findings  
164 of Chanson and Toombes (2001) for similar stepped spillway slopes. Without sidewalls, the  
165 lateral expansion also produces an increase in mean air concentration across the chute.

166

167 Figure 9 shows the evolution for normalized mean air concentration along the spillway ( $L/L_t$ ) for  
168  $(y_c/h)_e=2.37$ . As the flow is transversally expanding, the specific discharge decreases and mean  
169 air concentration increases, reaching maximum values of around  $1.3 \cdot (C_{med})_{qe}$ , where  $(C_{med})_{qe}$  is  
170 the mean air concentration at the spillway axis ( $x/B=0$  and  $1/30$ ), where the flow behaves like a  
171 conventional stepped spillway with sidewalls.

172

173 Figure 10 shows measurements of air concentration profiles lengthwise ( $L/L_t=0.95$  and  
174  $L/L_t=0.51$ ) and crosswise ( $x/B=0, 1/30, 1/10$  and  $1/6$ ). These profiles are also compared with  
175 Equation (4) proposed by Chanson and Toombes (2001). This equation shows a good agreement  
176 in the zone close to the free surface ( $y/y_{90}<0.40$ ), but does not fit well in the zone close to the  
177 pseudo-bottom ( $y/y_{90}>0.40$ ). This air profile behavior was also observed in conventional stepped  
178 spillways with sidewalls by Gonzalez (2005) and Renna et al. (2005).



### 179 3.6. Pressure field

180 In this study, pressures were obtained on the step footprint at a distance  $y/l=0.4$  from the external  
181 edge. The main aim of this section is to determine the pressure trends along and across the  
182 spillway due to flow spread. Figure 11 shows the transversal evolution ( $x/B$ ) of dimensionless  
183 mean pressure ( $p/\gamma h$ ) on the step footprint. Each figure provides information on longitudinal  
184 behavior ( $L/L_t$ ). From the results, for larger discharges mean pressure shows an increase across a  
185 step ( $x/B$ ). On the other hand, mean pressure decreases for points further away from the zone not  
186 affected by flow expansion ( $x/B=0$ ) and the lower mean pressure values are found closer to the  
187 spillway toe ( $L/L_t=0.95$ ).

188

189 In Figure 12, the crosswise and lengthwise evolution of mean pressures are normalized using  
190 mean pressure records for the zone that behaves like a stepped spillway with sidewalls,  $(p)_{qe}$ .  
191 There is a drop in the mean pressure registered across the chute due to transversal decrease in the  
192 specific discharge. A 50% reduction in the specific discharge produces a drop of 75% in mean  
193 pressure.

194

195 As expected, crosswise reduction of specific discharge is accompanied by a reduction of mean  
196 pressure over the stepped spillway. Specifically, for the maximum tested discharge  $(y_c/h)_e=2.37$ ,  
197 a 50% crosswise reduction produces a 75% reduction in mean pressure. Similarly, the further  
198 upstream, the lower the effect of the flow's lateral expansion for higher discharges at the entrance  
199 of the chute, and therefore the lower the pressure reduction.

## 200 4. Conclusions

201 This paper is framed within research work developed in response to a consulting partner's design  
202 of a stepped spillway without sidewalls. Studying the physical model has made it possible to  
203 determine the discharge distribution across and along the spillway. The velocity profiles, air  
204 concentration and water depths obtained lengthwise and crosswise of the spillway provide a

205 detailed description of the hydraulic effect of the water expansion as a result of the lack of  
206 sidewalls. Some results can be highlighted here:

207 – As the flow expands, both specific discharge and characteristic depth decrease. A 50%  
208 reduction in specific discharge means a 40% reduction in characteristic depth.

209 – On the other hand, as the flow expands, the specific discharge decreases, but mean air  
210 concentration increases between 1.2 and 1.3 times the air concentration in a stepped spillway  
211 with sidewalls.

212 – For the skimming flow regime, power  $N$  of the velocity profile law ranges between 3 and 5  
213 and increases as specific discharge diminishes. However, if specific discharge is low enough  
214 to become a transition flow,  $N$  doubles.

215 – The behavior of the air concentration profiles is similar to that in stepped spillways with  
216 sidewalls. The equation (4) by Chanson and Toombes (2001) fits well in the zone close to the  
217 free surface ( $y/y_0 \geq 0.40$ ).

218 – A 50% reduction in the flow rate produces a reduction of around 75% in mean pressures on  
219 the step's center of symmetry.

## 220 **5. Acknowledgements**

221 To the Spanish Ministry of Science and Innovation for supporting the proposal presented to the  
222 National Applied Research Projects under the National framework of R+D+I 2008-2011.

223

224 To Dragados S.A. (Group ACS) for their contribution in executing the collaborative applied  
225 research project, and to the Center for Hydrographic Studies, belonging to the Center of Studies  
226 and Experimentation (CEDEX), Spain.

227

228 To the Ecuadorian National Secretary of Higher Education, Science, Technology and Innovation  
229 (SENESCYT) for the financial support provided for Soledad Estrella Toral's PhD studies.

230

## 231 6. References

- 232 Amador, A. (2005). “Comportamiento hidráulico de los aliviaderos escalonados en presas de  
233 hormigón compactado.” Universitat Politècnica de Catalunya Barcelona-TECH.
- 234 Amador, A., Sánchez-Juny, M., and Dolz, J. (2006a). “Diseño hidráulico de aliviaderos  
235 escalonados en presas de HCR.” *Ingeniería del Agua*, 13(4), 289–302.
- 236 Amador, A., Sánchez-Juny, M., and Dolz, J. (2006b). “Characterization of the nonaerated flow  
237 region in a stepped spillway by PIV.” *Journal of Fluids Engineering*, 128(6), 1266–1273.
- 238 Amador, A., Sánchez-Juny, M., and Dolz, J. (2009). “Developing Flow Region and Pressure  
239 Fluctuations on Steeply Sloping Stepped Spillways.” *Journal of Hydraulic Engineering*,  
240 ASCE, American Society of Civil Engineers, Dept. of Hydraulic and Environmental  
241 Engineering, Technologic School of Barreiro, IPS, 2830-144 Barreiro, Portugal, 135(12),  
242 1092–1100.
- 243 Boes, R. M., and Hager, W. H. (1998). “Fiber-optical experimentation in two-phase cascade  
244 flow.” *Proc. Intl. RCC Dams Seminar*, K. Hansen, ed., Denver.
- 245 Boes, R. M., and Hager, W. H. (2003). “Two-phase flow characteristics of stepped spillways.”  
246 *Journal of Hydraulic Engineering*, ASCE, 129(9), 661–670.
- 247 Boes, R. M., and Minor, H.-E. (2001). “Inception point characteristics of stepped spillways.”  
248 *XXIX IAHR Congress*, Beijing, China.
- 249 Chanson, H. (1994). “Hydraulics of skimming flows over stepped channels and spillways.”  
250 *Journal of Hydraulic Research-IAHR*, 32(3), 445–460.
- 251 Chanson, H. (2001). “Hydraulic design of stepped spillways and downstream energy  
252 dissipators.” *Dam Engineering*, 11(4), 205–242.

- 253 Chanson, H., and Toombes, L. (2001). *Experimental investigations of air entrainment in*  
254 *transition and skimming flows down a stepped chute: application to embankment overflow*  
255 *on stepped spillways. Research Report No. CE158.* Dept. of Civil Engineering, The  
256 University of Queensland, Brisbane, Australia, 74.
- 257 Chanson, H., and Toombes, L. (2004). “Hydraulics of stepped chutes: The transition flow.”  
258 *Journal of Hydraulic Research*, 42(1), 43–54.
- 259 Chanson, H., Yasuda, Y., and Ohtsu, I. (2002). “Flow resistance in skimming flows in stepped  
260 spillways and its modelling.” *Canadian Journal of Civil Engineering*, 29(6), 809–819.
- 261 Estrella, S. (2013). “Comportamiento hidráulico de aliviaderos escalonados sin cajeros laterales  
262 en presas de HCR.” UPC BARCELONATECH, Barcelona.
- 263 Estrella, S., Sánchez-Juny, M., Dolz, J., and Ibáñez de Aldecoa, R. (2011). “Aliviaderos  
264 escalonados sin cajeros laterales.” *II Jornadas de Ingeniería del Agua 2011: modelos*  
265 *numéricos y dinámica fluvial.*
- 266 Falvey, H. T. (1980). *Air-water flow in hydraulic structures. Engineering Monograph No. 41,*  
267 *Department of the Interior, US Bureau of Reclamation, Denver Office, Water Resources*  
268 *Technical Publication, Denver, CO, US, 160.*
- 269 Gonzalez, C. A. (2005). “An experimental study of free-surface aeration on embankment  
270 stepped chutes.” University of Queensland, Australia.
- 271 Hunt, S. L., and Kadavy, K. C. (2013). “Inception Point for Embankment Dam Stepped  
272 Spillways.” *Journal of Hydraulic Engineering*, 139(1), 60–64.
- 273 De Marinis, G., Fratino, U., and Piccinni, A. F. (2001). “Flow regimes on stepped spillways.”  
274 *XXIX IAHR Congress, Beijing, China.*

275 Matos, J. (2000). "Hydraulic design of stepped spillways over RCC dams." *Hydraulics of*  
276 *Stepped Spillways*, H.-E. Minor and W. H. Hager, eds., Balkema, Rotterdam, VAW, ETH,  
277 Zürich, Switzerland, 187–194.

278 Matos, J., and Frizell, K. H. (2000a). "Air concentration and velocity measurements on self-  
279 aerated flow down stepped chutes." *Joint Conference on Water Resource Engineering and*  
280 *Water Resources Planning and Management 2000*, American Society of Civil Engineers,  
281 Minnesota, USA.

282 Matos, J., and Frizell, K. H. (2000b). "Air concentration and velocity measurements on self-  
283 aerated flow down stepped chutes." *Joint Conference on Water Resource Engineering and*  
284 *Water Resources Planning and Management 2000*, American Society of Civil Engineers,  
285 July 30-August 2, 2000. Minneapolis, Minnesota, USA.

286 Meireles, I. (2004). "Caracterização do escoamento deslizante sobre turbilhões e energia  
287 específica residual em descarregadores de cheias em degraus." Instituto Superior Técnico  
288 de Lisboa, Portugal.

289 Meireles, I., Renna, F., Matos, J., and Bombardelli, F. (2012). "Skimming, Nonaerated Flow on  
290 Stepped Spillways over Roller Compacted Concrete Dams." *Journal of Hydraulic*  
291 *Engineering*, 138(10), 870–877.

292 Peyras, L., Royet, P., and Degoutte, G. (1992). "Flow and energy dissipation over stepped  
293 gabion weirs." *Journal of Hydraulic Engineering, ASCE*, 118(5), 707–717.

294 Rajaratnam, N. (1990). "Skimming Flow in Stepped Spillways." *Journal of Hydraulic*  
295 *Engineering, ASCE*, 116(4), 587–591.

296 Relvas, A. T., and Pinheiro, A. N. (2011). "Velocity distribution and energy dissipation along  
297 stepped chutes lined with wedge-shaped concrete blocks." *Journal of Hydraulic*  
298 *Engineering, ASCE*, American Society of Civil Engineers (Hydraulics), 345 E. 47th St.

299 New York NY 10017-2398 USA, and ENGECONSULT, Consultores Técnicos Ltda,  
300 Rua Xavier Marques, 94, Afogados, Recife, CEP 52050-230, Brazil., 137(3), 423–431.

301 Renna, F., and Fratino, U. (2010). “Nappe flow over horizontal stepped chutes.” *Journal of*  
302 *Hydraulic Research*, 48(5), 583–590.

303 Renna, F., Fratino, U., and Matos, J. (2005). “Air-water flow features in skimming flow over  
304 steeply sloping stepped spillways.” *XXXI IAHR Congress*, 11-16 September 2005, Seoul,  
305 598–599.

306 Sánchez-Juny, M., Bladé, E., and Dolz, J. (2008a). “Pressures on a stepped spillway.” *Journal*  
307 *of Hydraulic Research-IAHR*, 46(4), 574–576.

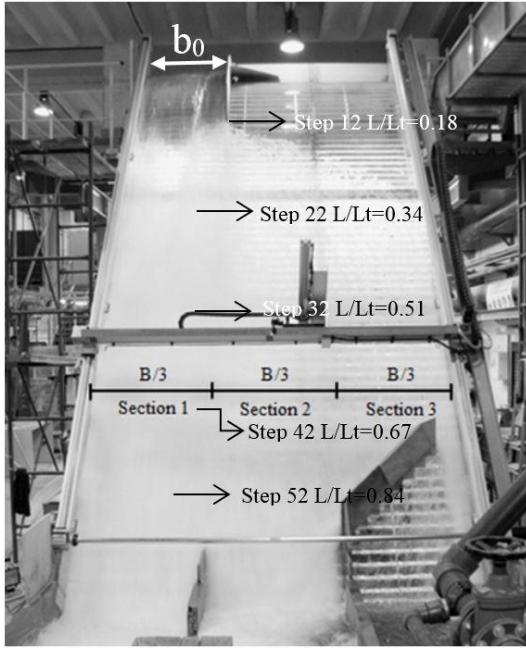
308 Sánchez-Juny, M., Bladé, E., and Dolz, J. (2008b). “Analysis of pressures on a stepped  
309 spillway.” *Journal of Hydraulic Research-IAHR*, 46(3), 410–414.

310 Sánchez-Juny, M., and Dolz, J. (2003). “Characterization of the pressure field over a stepped  
311 spillway in roller compacted concrete dams.” *In 4th Intl. Symposium on roller compacted*  
312 *concrete (RCC) dams*, L. Berga, J. M. Buil, C. Jofre, and S. Chonggang, eds., Balkema,  
313 Madrid (Spain), 697–700.

314 Sánchez-Juny, M., and Dolz, J. (2005). “Experimental study of transition and skimming flows  
315 on stepped spillways in RCC dams: Qualitative analysis and pressure measurements.”  
316 *Journal of Hydraulic Research-IAHR*, International Association of Hydraulic Engineering  
317 Research, Hydraulic Maritime and Environmental Engineering Department, UPC, Street  
318 Jordi Girona 1-3, 08034 Barcelona, Spain, 43(5), 540–548.

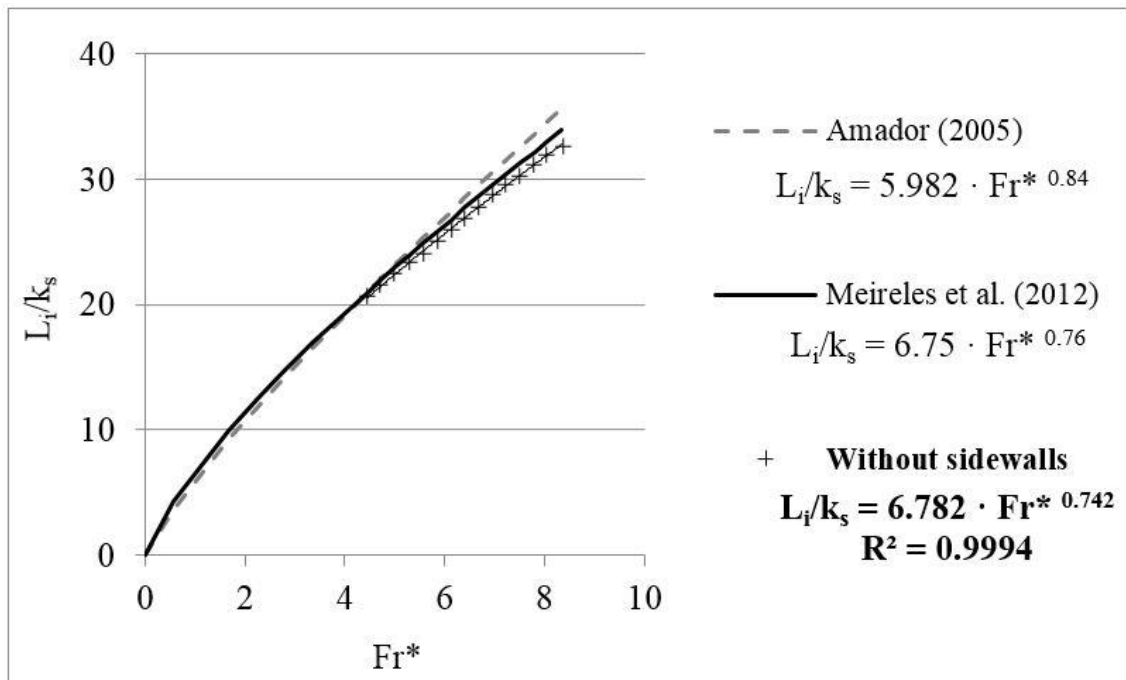
319

320



321

322 Figure 1. Front view of the stepped chute for a dimensionless specific discharge  $(y_c/h)_e=2.37$  and  
 323 a dimensionless spill-width  $b_0/B=1/3$ .



324

325 Figure 2. Comparison of the inception point observed without sidewalls and the equations  
 326 proposed by Amador et al. (2006a); Meireles et al. (2012) for the case with sidewall

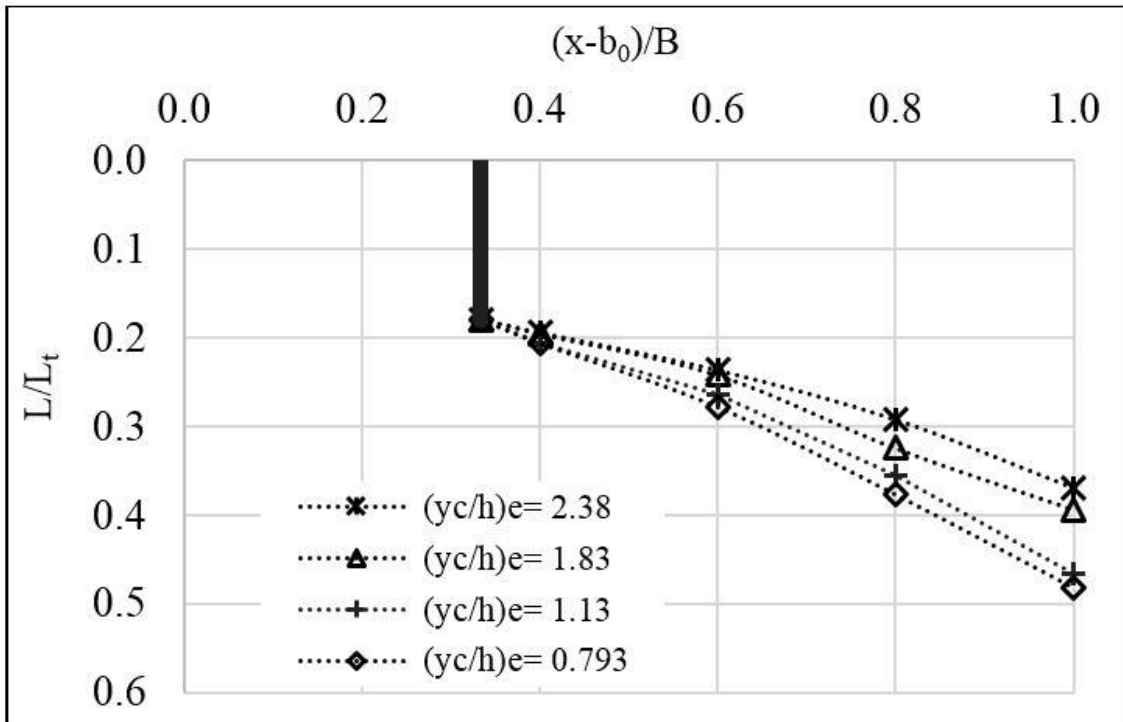
327

328

329

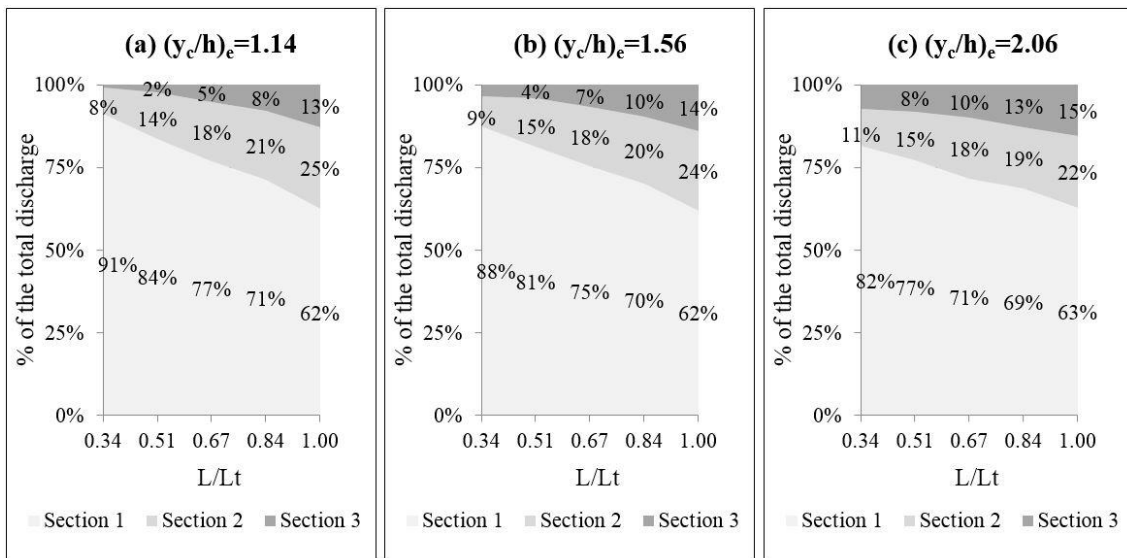
330

331



332

333 Figure 3. Lateral spread characterization along the spillway for different specific discharges at the  
 334 entrance

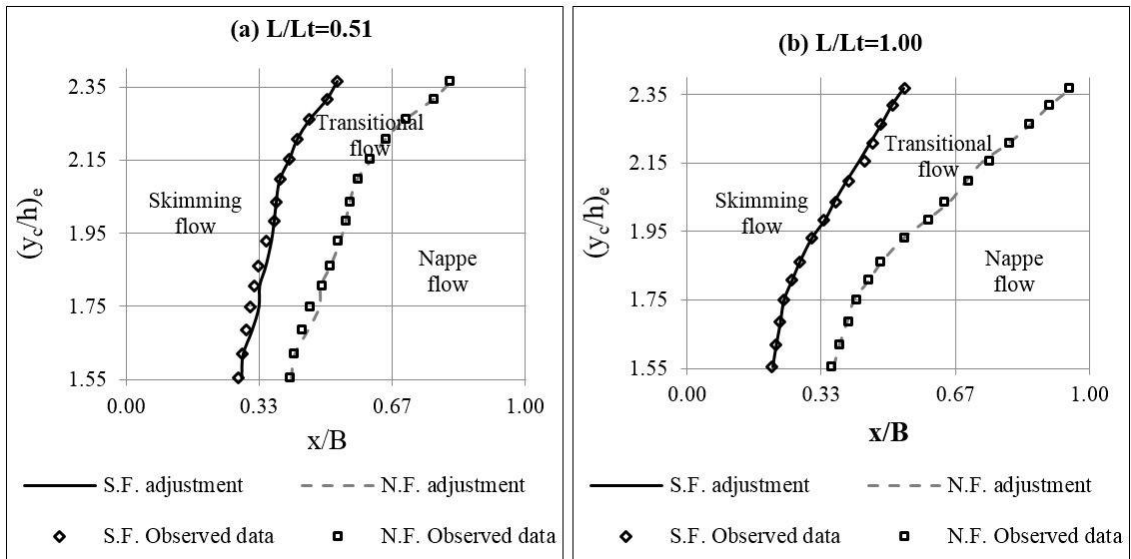


335

336 Figure 4. Flow distribution at a dimensionless distance along the chute obtained as the ratio  
 337 between the distance from the corresponding step to the crest (L), and the whole length of the  
 338 chute ( $L_t$ ), for the case  $b_0/B=1/3$ . (a)  $(y_c/h)_e=1.14$ , (b)  $(y_c/h)_e=1.56$ , (c)  $(y_c/h)_e=2.06$

339



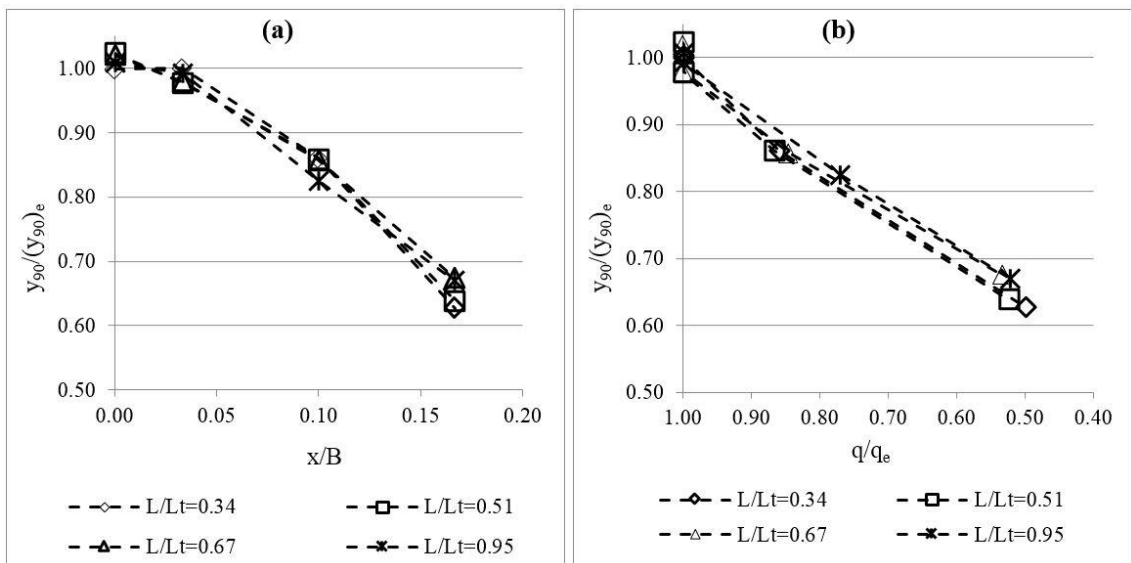


340

341 Figure 5. Crosswise flow regime characterization for  $(y_c/h)_e$  ranging between 1.55 and 2.37. S.F.

342 = inferior limit of skimming flow, N.F. = superior limit of nappe flow. (a) At the middle of the

343 spillway ( $L/L_t=0.51$ ), (b) At the spillway toe ( $L/L_t=1.00$ )



344

345 Figure 6. Evolution of normalized water depth along the spillway ( $L/L_t$ ), for  $(y_c/h)_e=2.37$ . (a)

346 Depending on transversal position ( $x/B$ ). (b) Depending on specific discharge ( $q/q_e$ )

347

348

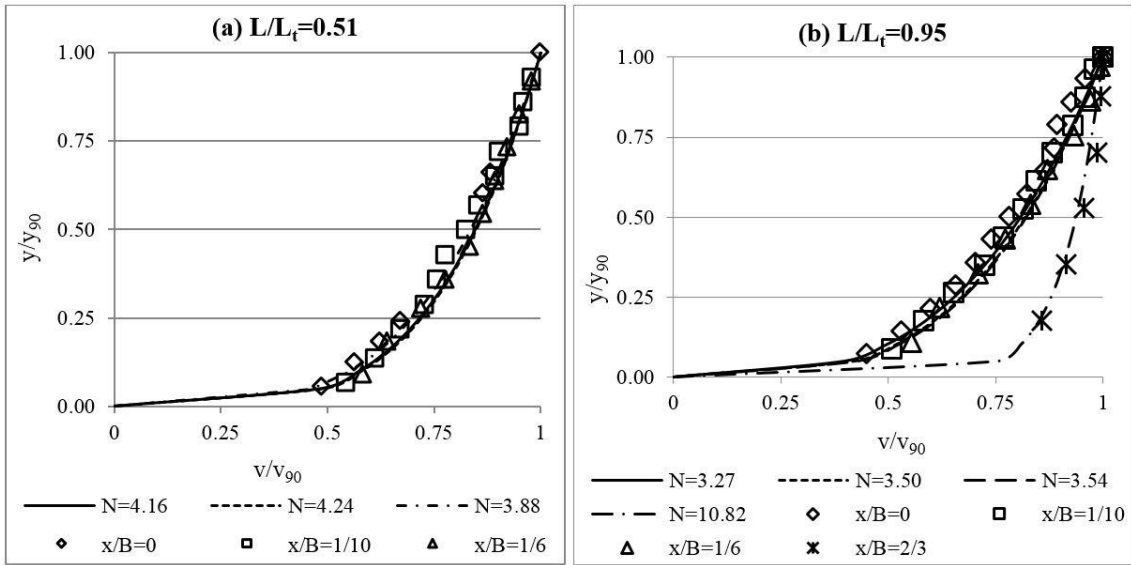
349

350

351

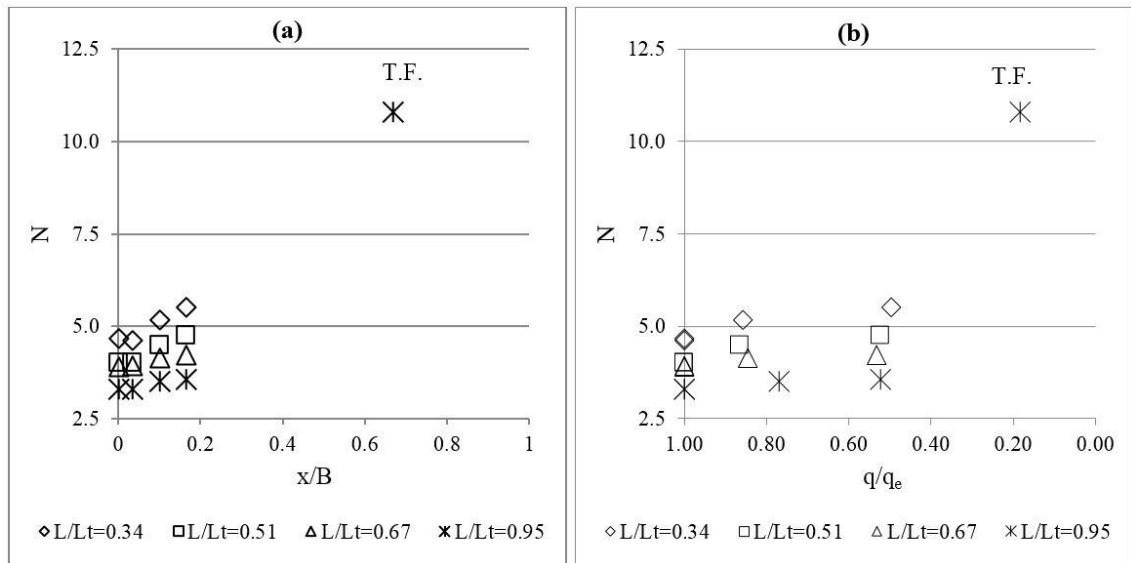
352

353



354

355 Figure 7. Normalized velocity profiles for  $(y_c/h)_e=2.37$  at (a)  $L/L_t=0.51$  and (b)  $L/L_t=0.95$ .



356

357 Figure 8. Lengthwise evolution ( $L/L_t$ ) of fitted coefficient  $N$ .  $(y_c/h)_e=2.37$ . T.F.=Transitional flow.

358 (a) Depending on transversal position ( $x/B$ ), (b) Depending on specific discharge ( $q/q_e$ ).

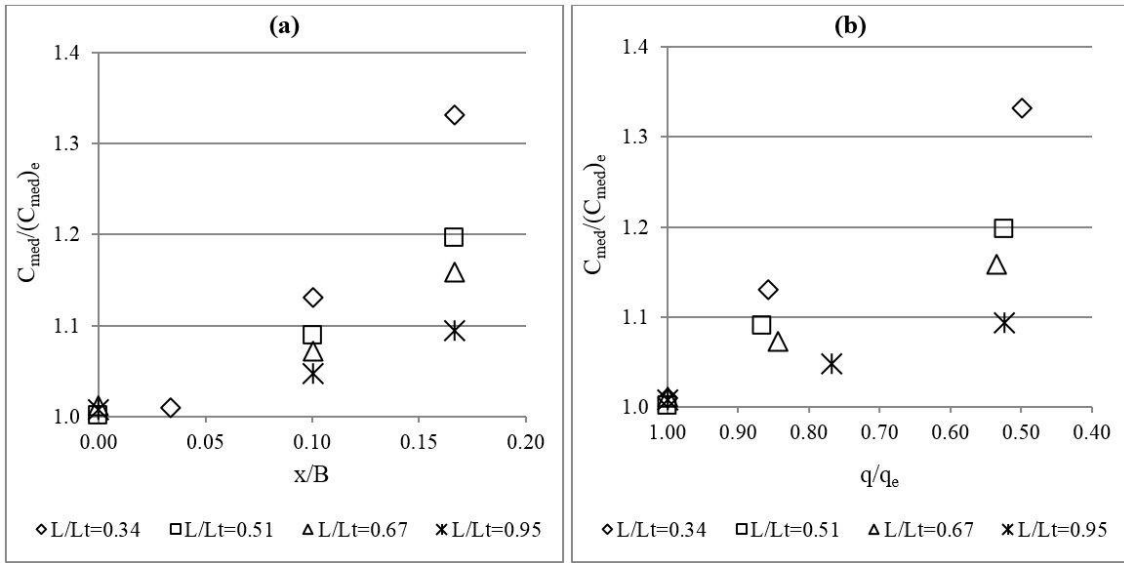
359

360

361

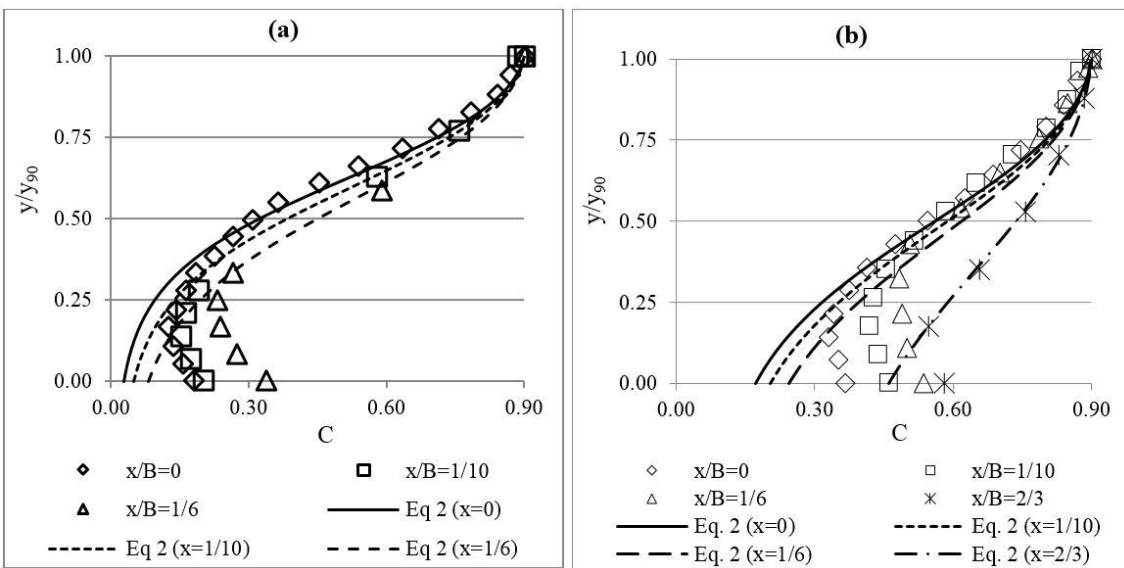
362

363



365

366 Figure 9. Lengthwise ( $L/L_t$ ) evolution of mean air concentration,  $(y_e/h)_e=2.37$ . (a) Depending on  
 367 transversal position ( $x/B$ ), (b) Depending on specific discharge ( $q/q_e$ )



368

369 Figure 10. Air concentration profiles for  $(y_e/h)_e=2.37$ , and comparison with the Equation (4)  
 370 proposed by Chanson and Toombes (2001). (a)  $L/L_t=0.51$ , (b)  $L/L_t=0.95$

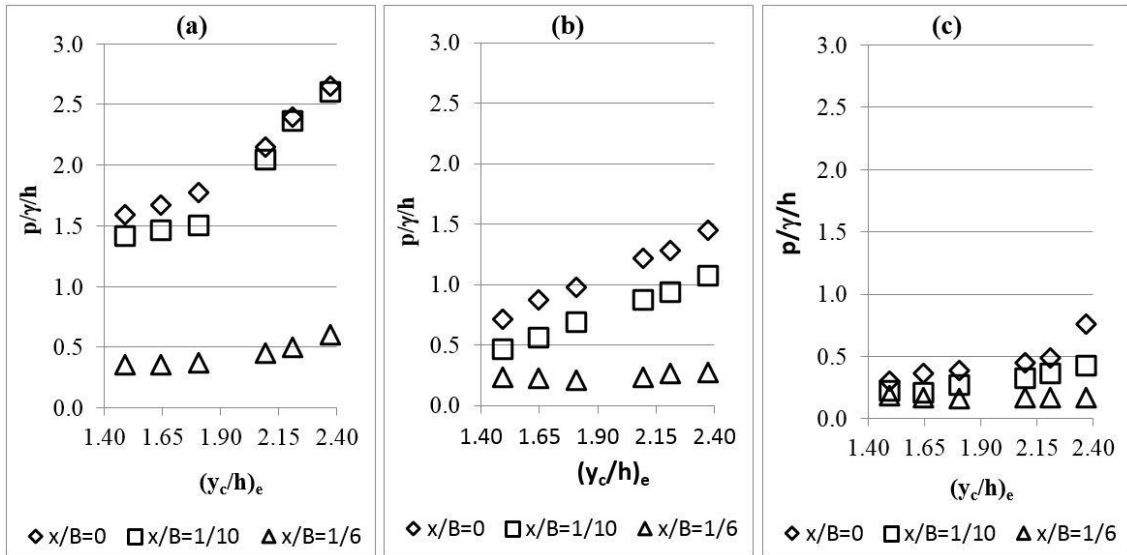
371

372

373

374

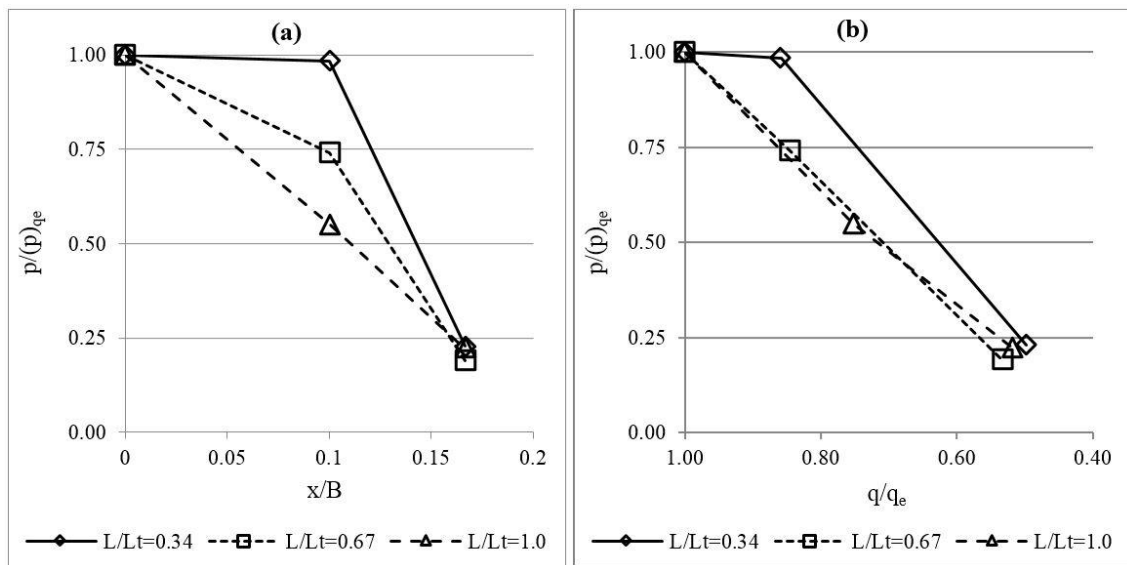
375



376

377 Figure 11. Evolution of dimensionless mean pressures lengthwise ( $L/L_t$ ) and crosswise ( $x/B$ ) the

378 spillway. (a).  $L/L_t=0.34$ , (b).  $L/L_t=0.67$ , (c).  $L/L_t=0.95$ .



379

380 Figure 12. Evolution dimensionless mean pressures for  $(y_c/h)_e=2.37$  at the spillway crest, for the

381 different heights  $L/L_t$ . (a) Crosswise evolution ( $x/B$ ). (b) Depending on  $q/q_e$ .

382

383